Liquid Crystals

Publication details, including instructions for authors and subscription information:
http://www.informaworld.com/smpp/title~content=t713926090

Spontaneous deformation of main-chain liquid-crystalline elastomers composed of smectic polyesters

Kazuyuki Hiraoka[a]; Tohru Tashiro[a]; Masatoshi Tokita[b]; Junji Watanabe[b]
[a] Center for Nano Science and Technology, Department of Nanochemistry, Tokyo Polytechnic University, Atsugi-shi, Japan [b] Department of Organic and Polymeric Materials, Tokyo Institute of Technology, Tokyo, Japan

To cite this Article Hiraoka, Kazuyuki , Tashiro, Tohru , Tokita, Masatoshi and Watanabe, Junji(2009) 'Spontaneous deformation of main-chain liquid-crystalline elastomers composed of smectic polyesters', Liquid Crystals, 36: 2, 115 — 122

To link to this Article: DOI: 10.1080/02678290802696165

URL: http://dx.doi.org/10.1080/02678290802696165

Liquid Crystals,
Vol. 36, No. 2, February 2009, 115–122

Taylor & Francis
Taylor & Francis Group

Spontaneous deformation of main-chain liquid-crystalline elastomers composed of smectic polyesters

Kazuyuki Hiraoka[a]*, Tohru Tashiro[a], Masatoshi Tokita[b] and Junji Watanabe[b]

[a]*Center for Nano Science and Technology, Department of Nanochemistry, Tokyo Polytechnic University, 1583 Iiyama, Atsugi-shi 243-0297, Japan;* [b]*Department of Organic and Polymeric Materials, Tokyo Institute of Technology, O-okayama, Mrguro-ku, Tokyo 152-8552, Japan*

(Received 29 October 2008; accepted 16 December 2008)

We observe the spontaneous shape change of a uniaxially deformed liquid-crystalline elastomer composed of smectic main-chain liquid-crystalline polyesters in a cyclic heating–cooling process. Although the elastomer contracts by about 115% on heating up to the isotropic phase, the sample length recovers by 55% on cooling to room temperature in the first heating–cooling process, and the elastomer exhibits an almost complete reversible deformation in the second heating–cooling process. By a comparison of the results of sample observation with those of X-ray analysis, we recognise that the strain λ was linearly coupled with the orientational order parameter S. In addition, the results of the X-ray analysis imply that a cybotactic nematic state, in which smectic clusters lie scattered in a nematic-like matrix, emerges after exposure to the isotropic phase.

Keywords: cybotactic nematics; elastomers; liquid-crystalline elastomers; liquid-crystalline polymers; polymer networks; shape memory; smectic clusters; smectic liquid crystals

1. Introduction

Liquid-crystalline elastomers have attracted both industrial and scientific interest because of their thermomechanical properties such as reversible strain actuation and soft elasticity (*1–10*). According to previous studies, the magnitude of deformation of liquid-crystalline elastomers is determined by coupling with the orientational order of mesogens and the conformation of polymer chains (*11–14*). Küpfer and Finkelmann have reported that a side-chain liquid-crystalline elastomer spontaneously elongates up to 40% = $((L–L_{\mathrm{iso}})/L_{\mathrm{iso}} \times 100)$ from the isotropic phase to the nematic phase, although the orientational order of mesogenic side chains is only indirectly coupled with the chain conformation in them (*12*). Here, L is the sample length and L_{iso} is the length in the isotropic phase. Main-chain liquid-crystalline elastomers have received increasing attention recently, because the direct coupling between the polymeric and mesogenic effects may bring a larger conformational change, which is expressed as high-performance thermomechanical behaviour (*15, 16*). Several years ago, Finkelmann and Wermter (*17, 18*) and Tajbakhsh and Terentjev (*19*) reported that nematic elastomers containing main-chain liquid-crystalline polymers have the remarkable property of being able to change their shape by up to more than 200% within a relatively narrow temperature interval straddling their isotropic–nematic (I–N) transition temperature.

Although there have been a few investigations on the reversible shape change of nematic main-chain liquid-crystalline elastomers, much less work has been carried out on those of smectics, in spite of their potentially useful mechanical properties attributable to their one-dimensional crystalline structure (*20, 21*). Recently, Sanchez-Ferrer and Finkelmann have reported that the tilt angle between the director and the layer orientation can be changed by the application of the mechanical field in smectic-C main-chain liquid-crystalline elastomers (*20*). Although their experimental results indicate a close coupling between the orientation of mesogens and the polymer conformation in smectic-C main-chain elastomers, the elastomers exhibited a small reversibility in the deformation in the heating–cooling process; although the change in length from the smectic phase to the isotropic phase is ΔL_{iso} = 208%, on cooling from the isotropic phase to the smectic phase, the unloaded sample only changes its length by ΔL_{iso} = 11% (see (*21*)).

Over the past two decades, Watanabe *et al.* have systematically studied the thermotropic mesomorphic properties of main-chain polyesters that are constructed by an alternative arrangement of the *p,p′*-bibenzoate unit as a mesogenic group and alkaneldiol as a flexible spacer (*22–25*). They reported that a homologous series of the polyesters, which are designated BB-*n*, where *n* is the number of methylene units in the diol, invariably forms smectic mesophases (*23*). In addition, the emergence of smectic mesophases has

---

*Corresponding author. Email: hiraoka@nano.t-kougei.ac.jp

ISSN 0267-8292 print/ISSN 1366-5855 online

DOI: 10.1080/02678290802696165
http://www.informaworld.com

recently been confirmed in polymer networks composed of BB-*n* polyesters (*25*). In this study, we have prepared uniaxially oriented smectic liquid-crystalline elastomers composed of BB-*n* polyesters with trifunctional crosslinkers and reported the deformation behaviour in a cyclic heating–cooling process, where successive phase transformations occur. Although the elastomer contracted by about 115% on heating from room temperature to the isotropic phase, the sample length recovered by 55% on cooling to room temperature in the first heating–cooling process. In addition, we have observed that once the elastomer was exposed to the isotropic phase it exhibited reversible shrinkage and elongation, estimated at about 50%, during the transformation between the isotropic and liquid-crystalline phases. Moreover, we have confirmed that the magnitude of deformation of the elastomers is linearly coupled with the orientational order parameter estimated by X-ray scattering observation.

2. Experimental details

2.1 Materials

An elastomer was synthesised by a melt transesterification of dimethyl *p,p′*-bibenzoate (1 mol) and a mixture of (*S*)-methylbutanediol (0.5 mol), hexanediol (0.5 mol) and 1,2,6- hexanetriol (0.1 mol). The chemical structures of these compounds are shown in Figure 1. The elastomer obtained is tentatively designated as a BB-4(2Me)/6-elastomer in this paper. Uniaxially ordered networks were obtained by applying the following multi-stage reaction. After the reaction was carried out at 230°C for 1 hour, the elastomer film cast was kept at 200°C for 1 hour. Thereafter, the film was deformed uniaxially by loading it with a stress of 50 mN mm^{-2} at 200°C for 24 hours. Here, dimethyl *p,p′*-bibenzoate was used as received from Ihara Chemical Co., Ltd. (S)-Methylbutanediol, hexanediol and 1,2,6-hexanetriol were also used as received from Tokyo Kasei Kougyo Co., Ltd. The liquid-crystalline elastomer showed the following phase sequence:

g – (38°C) – smectic phase – (215°C) – iso.

The smectic–isotropic transition temperature listed above was determined by differential scanning calorimetry (DSC) measurement (Seiko, SSC-500), which was carried out between room temperature and 270°C at a heating rate of 5°C min^{-1}. The smectic structure was confirmed by X-ray observation.

2.2 X-ray measurement

The molecular alignment of the elastomer was observed by X-ray measurement with a rotating anode X-ray system using a Cu-K$_\alpha$ beam filtered by a confocal mirror (λ = 1.54 Å, X-ray power = 2.7 kW). The measurement was performed using a two-dimensional image plate system (2540 × 2540 pixels, 50 μm resolution). The distance between the sample and the image plate was 100 mm. The sample was mounted in a microfurnace (Mettler, FP82HT), and a

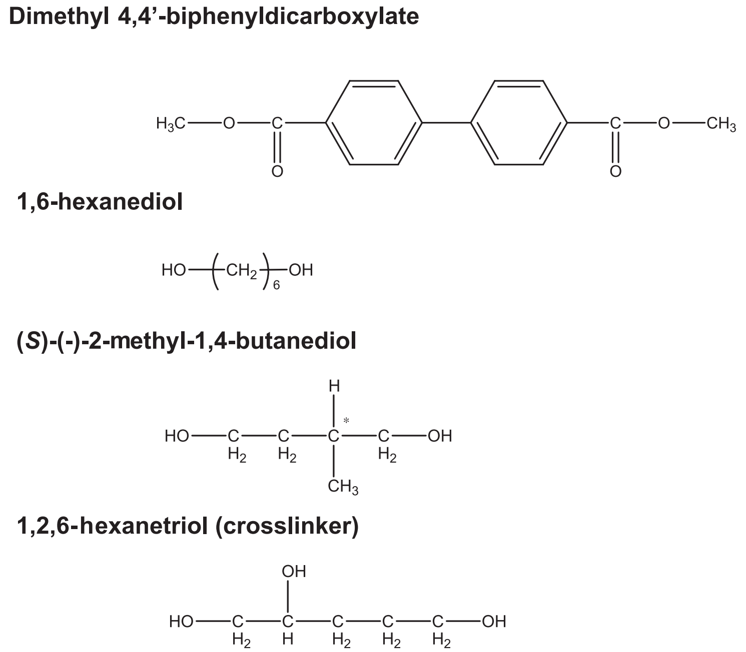

Figure 1. The system under investigation.

temperature-dependent X-ray measurement was carried out. The X-ray scattered on the *x*–*z* plane was measured after maintaining the measuring temperature for at least 10 min.

3. Results and discussion

We have observed the spontaneous shape change of the uniaxially deformed elastomer in a cyclic heating–cooling process between room temperature and the isotropic phase. Figure 2 shows photographs taken at room temperature and 230°C (isotropic phase) in the cyclic heating–cooling process. Here, the upper end of the elastomer is fixed to a sample holder, while the lower end is allowed to move freely. As mentioned in Section 2, the elastomer was uniaxially deformed parallel to the *z*-direction during the sample preparation. By comparing the photograph taken at room temperature (Figure 2(a)) with that in the isotropic phase (Figure 2(b)), we recognise that the elastomer shrinks in the heating process. As the elastomer spontaneously elongates in the cooling process after exposure to the isotropic state, the sample in Figure 2(c) becomes longer than that in Figure 2(b). In addition, shrinkage and elongation are also confirmed in the second heating–cooling process shown in Figures 2(c)– (e).

To estimate the magnitude of shape change, the strain $\lambda = L/L_{\mathrm{iso}}$ is plotted as a function of temperature in Figure 3. Here, the sample length L is defined as the distance between polyimide tapes, as depicted in Figure 2(a), and L_{iso} corresponds to the length in the isotropic phase. Here λ, which is estimated at 2.15 in the initial state of the elastomer at room temperature (arrow A in Figure 3), slightly decreases with increasing temperature in the temperature region of the smectic phase until about 200°C. For further increases in temperature, the elastomer shrinks rapidly because of the smectic–isotropic transition at about 220°C, while sample length is almost independent of temperature in the isotropic phase above 230°C. In the cooling process (open squares), a rapid elongation occurs during the isotropic–smectic phase transformation at about 220°C, and then λ slightly increases with further decreases in temperature and reaches 1.55 at room temperature (see arrow B). We should point out that sample length does not revert to its initial value after the first heating–cooling process.

Let us trace the change in λ in the second heating–cooling process in order to investigate the deformation behaviour of the elastomer exposed once in the isotropic phase. Here, λ in the second heating (filled triangles) follows a pass in the first cooling (open squares) in the temperature region observed. In the second cooling (open triangles), the elastomer elongates almost similarly to that in the first cooling, and then λ reaches 1.47 at room temperature. As 1.47 corresponds to 95% of the sample length before the second heating–cooling process ($\lambda = 1.55$), we may say that the smectic main-chain elastomer exhibits an almost completely reversible deformation in the second heating–cooling process.

To investigate molecular reorientation during the spontaneous deformation of the elastomer, we carried out a temperature-dependent X-ray measurement. An X-ray scattering pattern of the elastomer in the initial state at room temperature is shown in Figure 4(a), in which two characteristic reflections exist. Wide-angle reflection is associated with the molecular arrangement of the mesogenic side groups within smectic layers (arrow 1), and small-angle reflection is due to the smectic layers (arrow 2). The reflection at a wide angle, located near the equator, indicates the liquid-like arrangements of the macroscopic mesogens aligned macroscopically uniformly in the direction of the mechanical field parallel to the z-axis in Figure 4(a). An azimuthal intensity profile, which is achieved by scanning X-ray intensity, as displayed along the angle β (see Figure 4(a)), is shown in Figure 4(b). Since the wide-angle profile is well fitted to the Gauss distribution (see the solid line indicated by arrow 1 in Figure 4(b)), we are able to estimate the macroscopic order parameter $S = (1/2)\langle 3\cos^2\alpha_i - 1\rangle = 0.75$ (see (*26*)). Here, α_i is the angle between each molecular axis and the director. The azimuthal profile of the small-angle reflection (arrow 2 in Figure 4(b))

(a) r. t. (b) iso (c) r. t. (d) iso (e) r. t.

Figure 2. Photographs of uniaxially deformed smectic main-chain liquid-crystalline elastomer in a cyclic heating–cooling process.

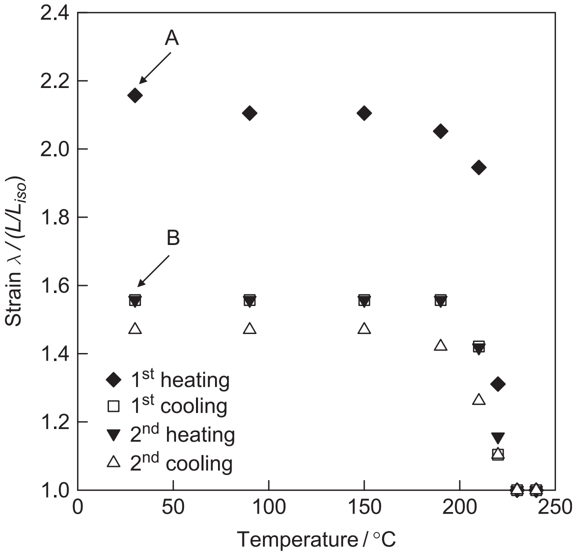

Figure 3. Temperature dependence of strain $\lambda = L/L_{\mathrm{iso}}$ of the uniaxially deformed smectic main-chain liquid-crystalline elastomer.

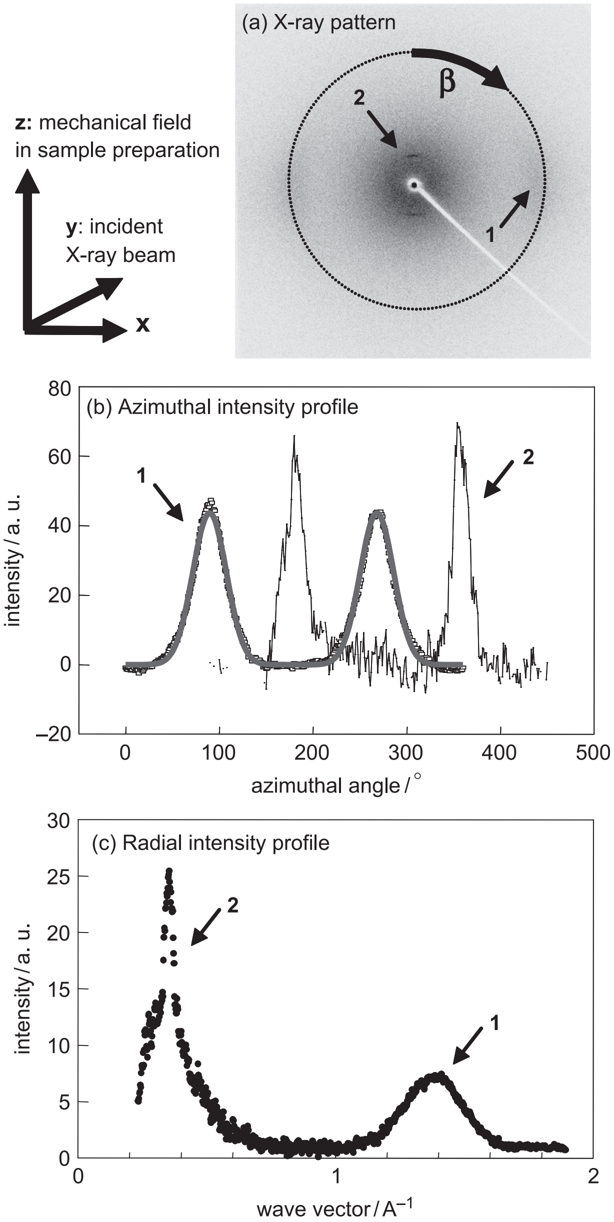

Figure 4. X-ray investigation of the uniaxially deformed smectic main-chain liquid-crystalline elastomer at room temperature: (a) X-ray scattering pattern; (b) azimuthal intensity profile; and (c) radial intensity profile.

indicates two maxima at the meridian position (at 180° and 360°), because the layer normal is parallel to the orientational director that describes the average direction of mesogens. The layer spacing, which can be estimated at about 17.8 Å on the basis of the radial intensity profile in Figure 4(c), was almost independent of temperature up to the smectic–isotropic transition temperature of 220°C. In addition, only a halo was observed in the X-ray pattern of the isotropic phase; no orientation was confirmed in the azimuthal profile.

Figure 5(a) shows an X-ray pattern of the elastomer after exposure to the isotropic phase. The X-ray pattern was taken at room temperature after cooling from the isotropic phase. Similarly to those observed in Figure 4(a), two characteristic reflections, namely the wide-angle reflection associated with the mesogenic side groups (arrow 1) and the small-angle reflection due to the smectic layers (arrow 2), are recognised. The azimuthal profile of the wide-angle reflection (arrow 1 in Figure 5(b)), in which two maxima are recognised at the equator position (at 90° and 270°), reveals that the mesogens are averagely reoriented parallel to the *z*-direction, namely, the direction of the uniaxially mechanical field during sample preparation. Fitting the profile to a Gaussian distribution (the solid line indicated by arrow 1 in Figure 5(b)), the order parameter *S* is estimated at 0.45. In other words, the average direction of the mesogens, namely, the direction of the director, is memorised even after exposure to the isotropic phase, although *S* does not reach its initial value of 0.75.

In order to estimate the change in molecular reorientation with varying temperature, the order parameter *S* is plotted as a function of temperature in Figure 6. Although *S*, which was estimated at 0.75 in the initial state at room temperature (arrow A in Figure 6), slightly decreases with increasing temperature in the smectic phase, it rapidly decreases at about 220°C where the transformation from the smectic phase to the isotropic phase occurs. In the first cooling (open squares), the order parameter *S* rapidly

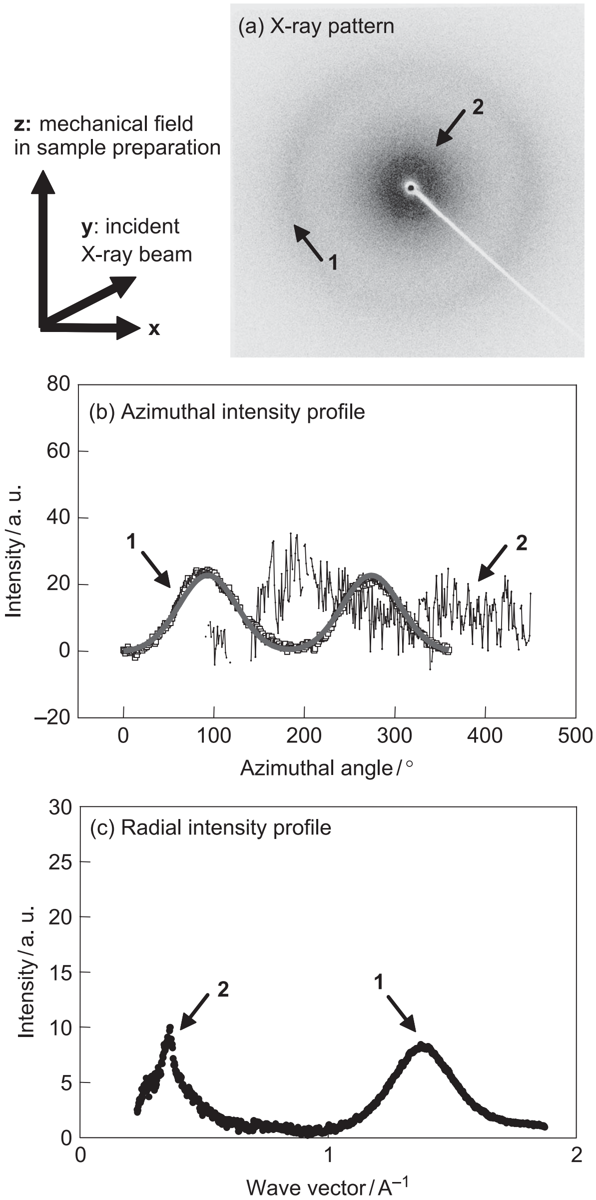

Figure 5. X-ray investigation of smectic main-chain liquid-crystalline elastomer after exposure to the isotropic phase: (a) X-ray scattering pattern at room temperature; (b) azimuthal intensity profile; and (c) radial intensity profile.

increases during the isotropic–smectic transformation at about 220°C. With further decrease in temperature, S slightly increases and reaches 0.45 at room temperature. The order parameter after exposure to the isotropic phase, namely, $S = 0.45$, is apparently lower than that in the initial state, because the order of orientation only partially recovers. In the second heating–cooling process, a rapid change in S is also observed during the smectic–isotropic (isotropic–smectic) transformation, and S slightly decreases (increases) with increasing (decreasing) temperature in the smectic temperature region. Note that S reverts to 0.45 after the second heating–cooling process (filled and open triangles). We may say that once the elastomer is exposed in the isotropic phase it acquires an almost complete reversibility in the orientational order of mesogens as well as in macroscopic deformation with varying temperature. By comparing the temperature dependence of the order parameter S (Figure 6) with that of the strain λ (Figure 3), we recognise that the change in S is closely associated with the magnitude of macroscopic deformation described by λ in the cyclic heating–cooling process. To quantitatively investigate the relationship between λ and S, λ is plotted as a function of S in Figure 7. We recognise the linear relationship ($S = 0.52 \cdot \lambda - 0.34$) between them similarly to those in previous reports dealing with the deformation of nematic elastomers (*11*, *12*, *17–19*). The linear relationship means that the shape change of the elastomer is coupled with the change in the orientational order of mesogens, which confirms the theoretical predictions in previous studies (*27*, *28*).

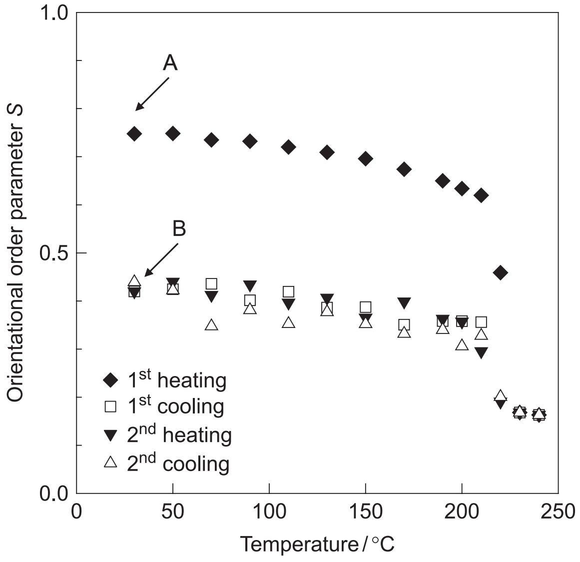

Figure 6. Temperature dependence of orientational order parameter S in cyclic heating–cooling process.

Let us return to the results of the X-ray analysis in Figures 4 and 5 to discuss the realignment of the layer structure in the cyclic heating–cooling process. The results of the X-ray analysis of the initial state of the uniaxially deformed elastomer (see arrow 2 in Figures 4(a) and (b)) indicate that both the director (average direction of mesogens) and the layer normal are parallel to the z-axis corresponding to the uniaxially mechanical field of sample preparation. As the smectic structure appears in cooling from the isotropic phase, the layer reflection can be recognised in the radial intensity profile, as indicated by arrow 2 in

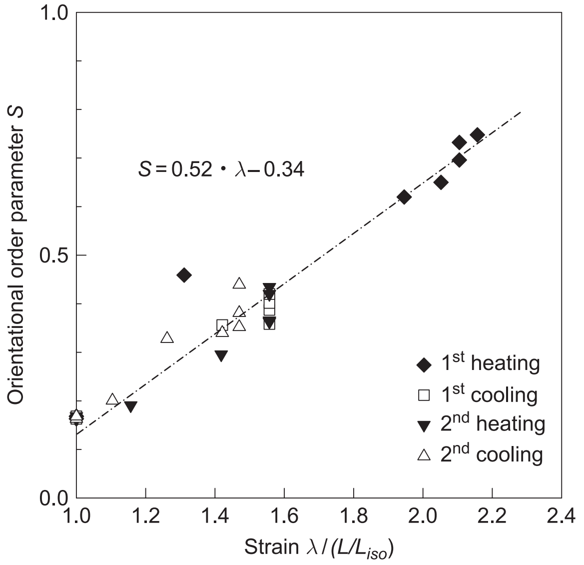

Figure 7. Relationship between orientational order parameter S and strain $\lambda = L / L_{\mathrm{iso}}$ of uniaxially deformed smectic main-chain liquid-crystalline elastomer. Measurements were carried out in a cyclic heating–cooling process.

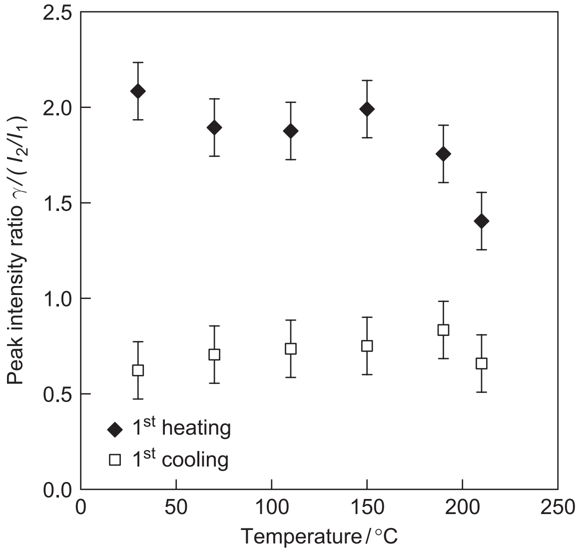

Figure 8. Temperature dependence of peak intensity ratio $\gamma = I_2 / I_1$, where I_2 is the intensity of layer reflection and I_1 is that of mesogenic reflection.

Figure 5(c). We should note that the azimuthal profile of the layer reflection of the elastomer once exposed to the isotropic phase is almost independent of the azimuthal angle, because the smectic layers are not oriented (arrow 2 in Figure 5(b)). As for the wide-angle reflection, however, the azimuthal profile (arrow 1 in Figure 5(b)) has indicated that the mesogens are averagely reoriented parallel to the z-direction, as we have mentioned above, because the uniaxial direction of mesogens is averagely memorised even after exposure to the isotropic phase. The contradiction between the layer alignment and the mesogenic orientation implies that non-oriented smectic layers and uniaxially oriented mesogens coexist. To explain the contradiction, we speculate a cybotactic nematic state in which smectic clusters lie scattered in a uniaxially oriented nematic-like matrix (see Figure 9(c) below) (*29–32*).

By comparing of the radial intensity profile in the initial state at room temperature (Figure 4(c)) with that after exposure to the isotropic phase (Figure 5(c)), we recognise the peak intensity ratio $\gamma = I_2 / I_1$, where I_2 is the intensity of layer reflection at small angle and I_1 is that of mesogenic reflection at wide angle, drastically decreases following exposure to the isotropic phase. Here, the intensity was calculated using the peak area. The decrease of γ indicates that the layer structure in the initial state is partially transformed into a nematic-like structure, which implies the emergence of the cybotactic nematic state. To investigate the structural change in the heating–cooling process, γ is plotted as a function of temperature in Figure 8. Although γ, which was estimated at about 2.1 in the initial state at room temperature, slightly decreases and reaches 1.4 at 210°C in the first heating process, for further increases in temperature, γ cannot be estimated above 220°C because of the smectic–isotropic transition. In the cooling process, the X-ray reflection peaks appear through the isotropic–smectic phase transition, and γ is estimated at about 0.66 just below the transition temperature. As the cybotactic nematic state emerges, as mentioned above, the value of γ falls to less than half of that measured before exposure to the isotropic phase. In addition, γ is almost independent of temperature in cooling, and it reaches about 0.62 at room temperature.

Consequently, let us illustrate the shape changes of the elastomer, namely, shrinkage and elongation, from the aspect of molecular reorientation in Figure 9 for further consideration of the spontaneous and reversible deformation of the elastomer. Figure 9(a) shows the molecular alignment in the initial state of the uniaxially deformed elastomer corresponding to the results of the X-ray analysis in Figure 4. Here, both the mesogens and the layer normal are uniaxially oriented parallel to the z-axis owing to the uniaxially mechanical field in sample preparation. As depicted in Figure 9(b), however, each orientational order almost disappears during the smectic–isotropic transformation, and sample shrinkage occurs simultaneously.

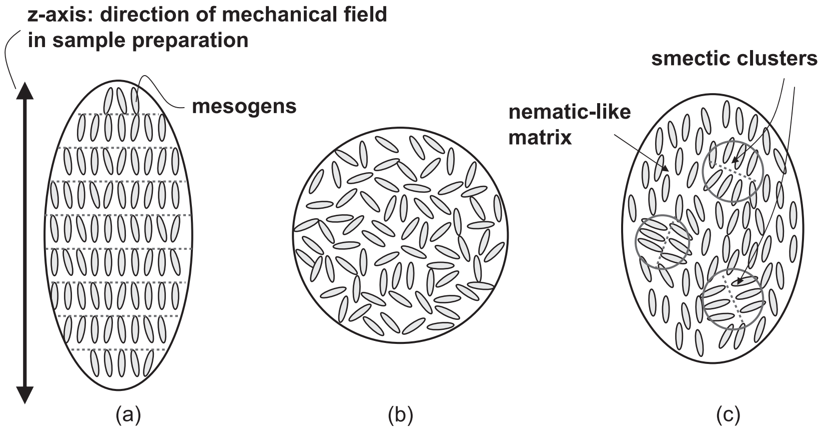

Figure 9. Schematic model describing molecular reorientation during isotropic–smectic phase transformation: (a) initial state at room temperature; (b) isotropic phase; and (c) room temperature after exposure to the isotropic phase.

In addition, sample elongation and an increase in the orientational order parameter *S* occur simultaneously in the first cooling from the isotropic phase to room temperature, although the sample length as well as the order parameter incompletely revert to the initial state. The X-ray pattern after the exposure to the isotropic state (Figure 5) indicates the coexistence of uniaxially oriented mesogens and non-oriented layers. Accordingly, we have speculated about the emergence of a cybotactic nematic state in which smectic clusters lie scattered in a uniaxially oriented nematic-like matrix, as depicted in Figure 9(c). As we have seen, the results of X-ray analysis and sample observation in the second heating–cooling process imply the molecular reorientation between Figures 9(b) and (c) is almost reversible. Owing to the linear coupling between the orientational order of mesogens, *S*, and the strain of the sample, λ, in Figure 7, we may say that it is not non-oriented smectic clusters but a uniaxially oriented nematic-like matrix that contributes to the reversible deformation of the elastomer. At present, we do not have sufficient information for further discussing the emergence of the cybotactic nematic state and its properties. In the meantime, we proceed to perform further experiments on the thermoelastic response as well as on the thermodynamic measurements of the smectic main-chain elastomers and hope to answer a number of questions about the emergence of the cybotactic nematic state. We will provide experimental details to confirm our hypothesis in the near future.

4. Conclusion

We have studied the shape change and molecular reorientation of a main-chain liquid-crystalline elastomer, which is composed of smectic main-chain liquid-crystalline polyesters, in a cyclic heating–cooling process where the smectic–isotropic (isotropic–smectic) phase transformation occurs. The sample used was a uniaxially oriented liquid-crystalline elastomer, which was obtained by uniaxial deformation during crosslinking. We observed spontaneous shape changes, namely, shrinkage and elongation, of the elastomer with varying temperature in the cyclic heating–cooling process. In the first heating–cooling process, the elastomer contracted by about 115% = $((L - L_{\mathrm{iso}})/L_{\mathrm{iso}} \times 100)$ on heating up to the isotropic phase, although the sample length recovered by only 55% on cooling to room temperature. In the second heating–cooling process, however, the elastomer exhibited an almost completely reversible deformation, in which the elastomer contracted and elongated by about 47–55%. As the macroscopic deformation of the elastomer resulted from the change in the orientational order of mesogens, the strain $\lambda = L/L_{iso}$ was linearly coupled with the orientational order parameter *S*. From the results of the X-ray analysis, which disclosed the coexistence of uniaxially oriented mesogens with non-oriented layers, we speculated that a cybotactic nematic state, in which smectic clusters lie scattered in a nematic-like matrix, emerged after exposure to the isotropic phase.

Acknowledgements

KH wishes to acknowledge valuable discussions with Dr Anke Hoffmann and Professor Dr Heino Finkelmann at ISMASM held at Awaji Island. We thank Dr Kensuke Osada for his advice about the synthesis of BB-*n* networks. We also thank Yasufumi Oka, Yuta Kato, Takehiro Nakamura and Ayumu Sagano for their experimental assistance. This work was supported by a Grant-in-Aid for Scientific Research (C) (#20550167) from the Ministry of Education, Culture, Sports, Science and Technology (MEXT), and also partially supported by the 'Academic Frontier Project' for private universities (2006–2008): matching fund subsidy from MEXT.

References

(1) Finkelmann, H.; Kock, H.J.; Rehage, G. *Makromol. Chem. Rapid Commun.* **1981**, *2*, 317.

(2) Zentel, R.; Reckert, G. *Makromol. Chem.* **1986**, *187*, 1915.

(3) Mitchell, G.R.; Devis, F.J.; Ashman, A. *Polymer* **1987**, *28*, 639.

(4) Brand, H.R.; Finkelmann, H. *Handbook of Liquid Crystals*, vol. 3, Demus, D., Goodby, J., Gray, G.W., Spiess, H.-W. and Vill, V., Eds.; Wiley-VCH: Weinheim, 1998, pp. 277–302.

(5) Zentel, R. *Angew. Chem. Adv. Mater.* **1989**, *101*, 1437.

(6) Devis, F.J. *J. Mater. Chem.* **1993**, *3*, 551.

(7) Barclay, G.G.; Ober, C.K. *Prog. Polym. Sci.* **1993**, *18*, 899.

(8) Warner, M.; Terentjev, E.M. *Liquid Crystal Elastomers*; Clarendon Press: Oxford, 2003, pp. 1–7, 93–106.

(9) Palffy-Muhoray, P. *Phys. Today*, **2007**, *60*, 54–60.

(10) Urayama, K. *Macromolecules*, **2007**, *40*, 2277.

(11) Schätzle, J.; Kaufhold, W.; Finkelmann, H. *Makromol. Chem.* **1989**, *190*, 3269–3284.

(12) Küpfer, J.; Finkelmann, H. *Makromol. Chem. Rapid Commun.* **1991**, *12*, 717.

(13) de Gennes, P.G. *C. R. Acad. Sci. Paris Ser. II* **1997**, *324*, 343.

(14) Thomsen, D.L.III; Keller, P.; Naciri, J.; Pink, R.; Jeon, H.; Shenoy, D.; Ranta, B.R. *Macromolecules* **2001**, *34*, 5868.

(15) Bergmann, G.H.F.; Finkelmann, H.; Percec, V.; Zao, M. *Macromol. Rapid. Commun.* **1997**, *18*, 353–360.

(16) Oritiz, C.; Wagner, M.; Bhargava, N.; Ober, C.K.; Kramer, E.J. *Macromolecules* **1998,** *31,* 8531–8539.

(17) Finkelmann, H.; Wermter, H. *ACS Abstracts* **2000**, *219*, 189.

(18) Wermter, H.; Finkelmann, H. *e-Polymers* **2001**, no. 013 (available at http://www.e-polymers.org/papers/finkelmann_ 210801.pdf).

(19) Tajbakhsh, A.R.; Terentjev, E.M. *Eur. Phys. J. E* **2001**, *6*, 181.

(20) Sanchez-Ferrer, A.; Finkelmann, H. *Macromolecules*, **2008**, *41*, 970–980.

(21) Rousseau, I.A.; Mather, P.T. *J. Am. Chem. Soc.* **2003**, *125*, 15 300–15 301.

(22) Kringbaum, W.R.; Watanabe, J. *Polymer*, **1983**, *24*, 1299–1307.

(23) Watanabe, J.; Hayashi, M.; Morita, A.; Tokita, M. *Macromolecules* **1995**, *28*, 8073–8079.

(24) Hiraoka, K.; Nose, T.; Uematsu, Y.; Tokita, M.; Watanabe, J. *Liq. Cryst.* **2007**, *34*, 305–310.

(25) Ishige, R.; Tokita, M.; Naito, Y.; Zhang, C.Y.; Watanabe, J. *Macromolecules* **2008**, *41*, 2671–2676.

(26) Mitchell, G.R.; Windle, A.H. *Developments in Crystalline Polymers 2*; Elsevier: Harlow, 1988, 115–175.

(27) Renz, W.; Warner, M. *Proc. R. Soc. London Ser. A* **1988**, *417*, 213.

(28) Clarke, S.M.; Hotta, A.; Tajbakhsh, A.R.; Terentjev, E.M. *Phys. Rev. E* **2001**, *64*, 061702.

(29) Lubensky, T.C.; Chen, J.H. *Phys. Rev. B*, **1997**, *1978*, 306.

(30) Isabel, K.; Finkelmann, H. *Macromol. Chem. Phys.*, **1998**, *199*, 677.

(31) Francescangeli, O.; Yang, B.; Laus, M.; Angeloni, A.S.; Galli, G.; Chielline, E. *J. Polym. Sci. B* **1995**, *33*, 699–705.

(32) Francescangeli, O.; Laus, M.; Galli, G. *Phys. Rev. E* **1997**, *55*, 481–487.